

Theoretical investigation of alkali-metal doping in Si clathrates

Alexander A. Demkov, Otto F. Sankey, and K. E. Schmidt

Department of Physics and Astronomy, Arizona State University, Tempe, Arizona 85287

Gary B. Adams and Michael O'Keeffe

Department of Chemistry and Biochemistry, Arizona State University, Tempe, Arizona 85287

(Received 25 May 1994)

The effects of doping Si clathrate structures with alkali metals have been investigated theoretically. We discuss (a) the electronic structure of Na and other alkali-metal-doped Si clathrates, and (b) the possibility of a Jahn-Teller effect. We also discuss band-gap engineering for Si materials, as well as Mott's conjecture for the electrical and magnetic properties of $\text{Na}_x\text{Si}_{136}$ clathrate compounds. We use the self-consistent plane-wave technique to study the electronic structure, and an *ab initio* tight-binding-like molecular dynamics is performed to determine geometries, energetics, and Jahn-Teller effects.

I. INTRODUCTION

Clathrate, or inclusion structures have been known for many years as hydrates of species such as chlorine and noble gases. They were mentioned by Davy, and shortly afterwards by Faraday in the early nineteenth century.^{1,2} A salient feature of such structures is a four-connected hydrogen-bonded network with large polyhedral cavities that accommodate the templating guest species. The same structures, now with Si-O-Si bonds replacing the O-H-O hydrogen-bonded network, have also been characterized as polyphorms of SiO_2 known as clathrasils, such as in the naturally-occurring melanophlogite. More recently, the same frameworks have been found for compositions Na_xSi ($x < 1$) prepared by careful decomposition of NaSi, etc.³ Now Na atoms are in polyhedral cavities of a four-connected Si framework.

The two most important clathrate frameworks are cubic, and in the context of hydrates are known as type I and type II. In an earlier paper, we have described these structures. The present paper is concerned with type II structure, both pure and with alkali-metal atoms incorporated in the structure. The pure Si structures I and II can be described as being composed of face sharing polyhedra, with Si atoms in the vertices. Each Si atom has four neighbors, just as it has in the diamond phase. To form a closed polyhedron one must satisfy the 12 pentagon rule, just as for fullerenes. Thus, the smallest possible polyhedron is a 20 atom pentagonal dodecahedron, shown in Fig. 1(a). Keeping the number of pentagonal faces fixed, we add hexagonal rings to form a tetrakaidecahedron (two hexagons) and a hexakaidecahedron (four hexagons) as shown in Figs. 1(b) and 1(c), respectively. These three polyhedra are the building blocks of the clathrate structures. An infinite periodic lattice may be formed by arranging the polyhedra in the following ways. The tetrakaidecahedra are first stacked by sharing hexagons to form infinite rods. These rods are then packed to form a simple cubic structure

where internal voids turn out to be pentagonal dodecahedra. The resulting type I structure is simple cubic with 46 Si atoms per unit cell. We referred to that structure as Si(46) in the earlier paper. Alternatively, a face-centered-cubic (fcc) type II structure can be formed if one uses hexakaidecahedra and dodecahedra as building blocks. This structure has 136 atoms in the cubic cell or 34 atoms in the primitive cell. We referred to that structure as Si(34). Our present work is concerned with that structure. When alkali-metal atoms are present, we will use the formula $M_n\text{Si}_{136}$ to indicate that the cubic unit cell contains n M atoms (where $M = \text{Na}, \text{K}, \text{etc.}$) and 136 Si atoms. For example, $\text{Na}_4\text{Si}_{136}$ means that there are four Na atoms in the cubic 136 atom cell.

Recently, the group IV elemental semiconductors Si and C in the clathrate structure have been studied both experimentally and theoretically by several groups, including ours.⁴⁻⁶ The Si clathrate solids were examined experimentally by Roy *et al.*,⁴ who being encouraged by the recent discoveries of superconductivity in carbon fullerene compounds, began searching for superconductivity in Si-Na systems. No high transition temperature was found. Our group has recently examined the energetics and band structures of the elemental semiconductor Si (without alkali metals) in two different four-coordinated clathrate structures.⁵ In that work, *ab initio* tight-binding-like molecular dynamics calculations, and fully self-consistent plane-wave calculations were performed. It was predicted that the energies of these structures were only slightly above that of the ground state diamond structure (by ≈ 0.07 eV/atom), and that they had an indirect band gap of about 1.9 eV, i.e., about 0.7 eV larger than that of Si in the diamond structure. In addition, Nesper *et al.*⁶ have performed similar calculations on pure carbon in clathrate (and other zeolite) structures. Their local density approximation calculations show these carbon structures are also very low in energy – substantially lower in energy than the fullerene molecule C_{60} , and lower in energy than polybenzene, a low energy,

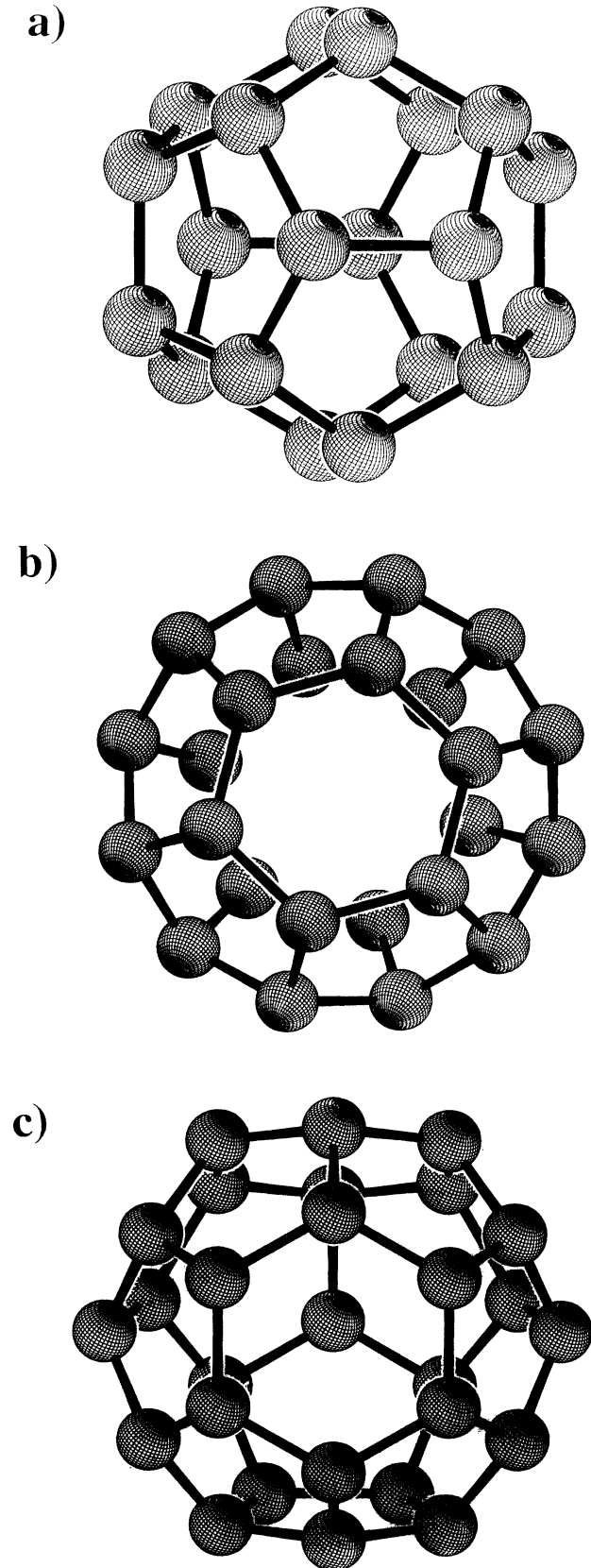


FIG. 1. The building blocks of the silicon clathrate structures: (a) pentagonal dodecahedron, (b) tetrakaidecahedron, and (c) hexakaidecahedron.

three-coordinated, sp^2 -bonded, three-dimensional hypothetical carbon network.⁷

There are striking similarities between the Si-Na clathrates and the alkali-metal-doped C_{60} fullerene solids. In both structures, the building blocks are rather large polyhedra — the 60 atom icosahedron in the case of carbon; and the 20 atom dodecahedron and the 28 atom hexakaidecahedron in the case of Si(34) clathrate. Both systems undergo an insulator-to-metal transition upon doping with alkali metals.^{4,8} However, there is a significant difference between the two groups of materials in their bonding. Within the fullerene solid, the crystal is held together *via* weak van der Waals type interactions and the carbon polyhedra retain strong molecular features. The silicon clathrates are *bona fide* covalent solids. As far as doping with alkali metals is concerned, in fullerenes the dopant atoms are interstitial outside the polyhedra, whereas in clathrates they occupy interstitials within the polyhedra. Experimentally, the magnetic susceptibility disappears in Na_xSi_{136} when x reaches approximately 8, probably due to a transition from an insulator to a metal.⁴ This composition is interpreted to be the composition in which every hexakaidecahedron is fully occupied. At lower Na concentrations the EPR measurements indicate the presence of well-separated Na atoms, and allow tracking of electron delocalization with increasing Na concentration. The first qualitative description of the insulator-to-metal transition in Si clathrates was given by Mott,⁹ in his interpretation of earlier experiments by Cros *et al.*¹⁰

In this paper, we take Si(34) clathrate solid as the model Si clathrate system, and address the following points: (a) the effects on the electronic structure due to Na and other alkali-metal doping, and (b) the Jahn-Teller (JT) effect. Finally, Mott's conjecture concerning the insulator to metal transition for the electrical and magnetic properties of Na_xSi_{136} compounds is reevaluated.

II. ALKALI METALS IN CLATHRATES— Na_4Si_{136} AND Na_8Si_{136}

The band structure of Si(34) predicted by a self-consistent plane-wave calculation within the local density approximation (LDA) was reported in Ref. 5 [see Fig. 4(b) of that reference]. The band gap is indirect, but is widened by more than 0.7 eV compared to a similar calculations of Si in the diamond structure. This is the limiting case ($x=0$) in the family of compounds of the type Na_xSi_{136} . We now investigate the effect of Na doping on the band structure. To investigate this we must first specify how the alkali-metal atoms are incorporated into the clathrate structure. A description of the clathrate phase geometry is given in (Ref. 5), and for the purpose of the current discussion, it is only important to recall that there are eight large hexakaidecahedra and 16 small dodecahedra per unit cell. The metal atoms may occupy interstitial sites within some or all polyhedra depending on concentration. It is known experimentally that in these compounds Na atoms occupy the largest polyhedra first.⁴ No study of Na atoms ordering in the

structure has yet been reported. Two special cases are the compound $\text{Na}_8\text{Si}_{136}$ with all of the hexakaidecahedra occupied by Na, and all of the dodecahedra empty, and the $\text{Na}_4\text{Si}_{136}$ compound with only half of the interstitial sites occupied.

First, we consider the case when $x = 4$. We assume that every other hexakaidecahedron in the unit cell is occupied (perfect order). This means that the sodium atoms are on an fcc crystal lattice and the symmetry is $F\bar{4}3m$. A Na atom is in a site of $\bar{4}3m = T_d$ symmetry as shown in Fig. 2. We perform a self-consistent band structure calculation using a plane-wave expansion within the local density approximation and the pseudopotential approximation. Soft pseudopotentials of the Kerker-Martins-Troullier type^{11,12} are used and the plane-wave energy cutoff is chosen to be 200 eV. The integration over the Brillouin zone, to obtain the charge density and the total energy, is done using two special k points in the irreducible wedge. The resulting band structure in the near-band-gap region is shown in Fig. 3. The most striking feature of the band structure is the absence of any new states in the gap. The highest occupied band, near 1.2 eV, is approximately half occupied by a single electron (from Na), and has very little dispersion (≈ 0.2 eV). It is triply degenerate at the Γ ($k = 000$) point. Note that the degeneracy at the (110) and (100) k points has been lifted, compared to that of pure Si. Also note that at the Γ point, the higher energy singly degenerate conduction band state at about 0.3 eV above the conduction band minimum was nearly 1.0 eV above the conduction band minimum in pure Si. Thus, the effect of Na is to flatten the lowest conduction band (which is triply degenerate at the Γ point), and to substantially lower the higher energy state which is singly degenerate at Γ .

In order to gain some insight into the physics of these states, we have performed model calculations using a modification of the local-orbital density functional method of Sankey and Niklewski.¹³ This local-orbital picture has the advantage of being easier to interpret.

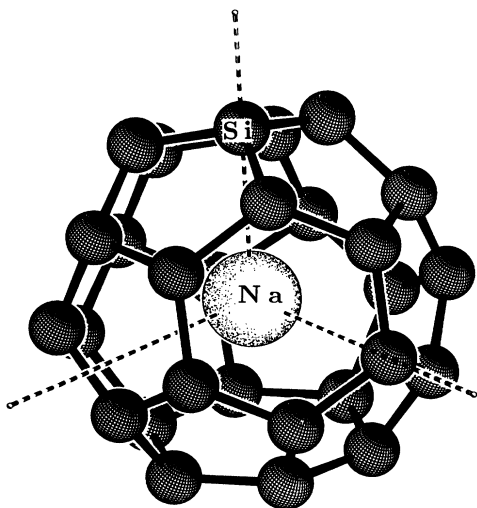


FIG. 2. A Na atom in the center of the Si hexakaidecahedron. This site has a perfect T_d symmetry.

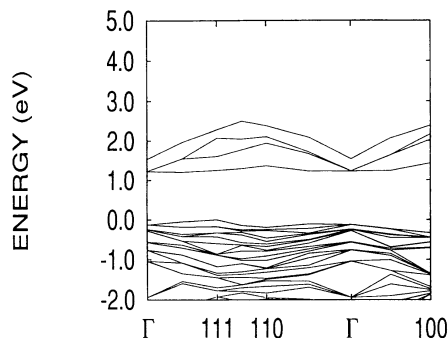


FIG. 3. The band structure in the near-band-gap region of $\text{Na}_4\text{Si}_{136}$ computed using plane waves.

We mimic the effect of alkali-metal doping using a “pseudoatom” technique by inserting an extra Si atom in the center of every other hexakaidecahedron (ordered $\text{Na}_4\text{Si}_{136}$), just as we introduced the Na atom in the plane wave calculation. The distance from this “interstitial” to the first neighbor is near the second nearest neighbor distance in diamond phase Si ≈ 3.8 Å. Because of this large distance, we introduce little error in setting to zero the overlap (which gives a second order correction) between the simulated atom in the center of the cage and the remainder of the system. This was checked by independent calculations which included the overlap with the result being very close quantitatively. The diagonal s and p matrix elements on the “pseudoatom” are now shifted upward in unison to simulate an electropositive element like Na; when the shift is large the atom is electronically removed and the system reverts back to the ideal Si clathrate band structure. For smaller shifts (less than +10 eV) the interstitial is more alkali-metal like. For example, Hartree-Fock calculations yield the energy difference between the $3s$ state of silicon and $3s$ state of sodium to be 9.7 eV,¹⁴ while the LDA gives 8.1 eV for this difference.

First, we study the behavior of the eigenstates in the near-gap region at the Γ point as a function of the on-site energy shift of the interstitial atom from Si. Results are shown in Fig. 4. An A_1 state (s like) is pulled down

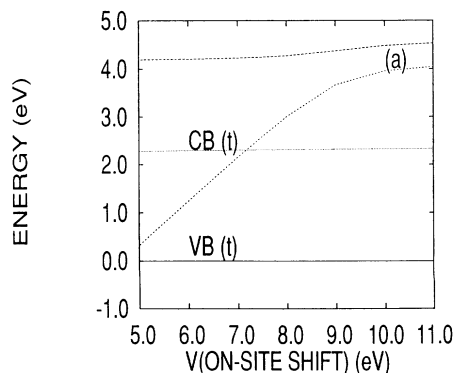


FIG. 4. The eigenstates in the near-gap region at the Γ point as a function of the on-site energy shift $\Delta V_{\text{on-site}}$ of the interstitial atom from Si.

from the conduction band as the on-site shift is reduced, while the triply degenerate T_2 states at the bottom of the conduction band are unaffected. The largest slope of the A_1 energy curve is ≈ 0.9 , suggesting a very high degree of localization of the wave function on the interstitial. From a comparison with the energy splitting between the T_2 and the A_1 conduction band states in the self-consistent plane-wave calculation (Figs. 3), we conclude that an on-site shift in the range from 7.5 to 8.0 eV adequately represents sodium, in accord with Hartree-Fock and LDA atomic calculations. An on-site shift of 7.5 eV gives the A_1 - T_2 splitting at the Γ point closest to that of the plane-wave calculation, while the shape and width of the lowest conduction bands are reproduced better with the 8.0 eV shift.

This technique gives us a powerful tool to investigate effects of alkali-metal doping on the electronic structure

of silicon clathrates, since by changing the on-site energy shift we can approximately "scan" through the periodic table. The evolution of the band structure with the on-site shift is shown in Fig. 5. As one can see, the main changes take place in the lower conduction band. The atomic states associated with the interstitial atom lie higher in the conduction band. For on-site shifts bigger than 10 eV the lowest conduction band still retains the features of pure Si(34) [Fig. 5(a)]. For a shift of 10.0 eV (this shift may be interpreted as a "pseudo-K"), the lowest conduction band begins to change and the degeneracy at (110) and (100) k points is noticeably broken [Fig. 5(b)]. At a shift of 8.0 eV [Fig. 5(c)], the lowest conduction band becomes relatively flat (dispersion is about 0.2 eV), and at 7.5 eV [Fig. 5(d)] we have an almost flat band that is triply degenerate at the Γ point. As discussed above, this shift may be interpreted as a

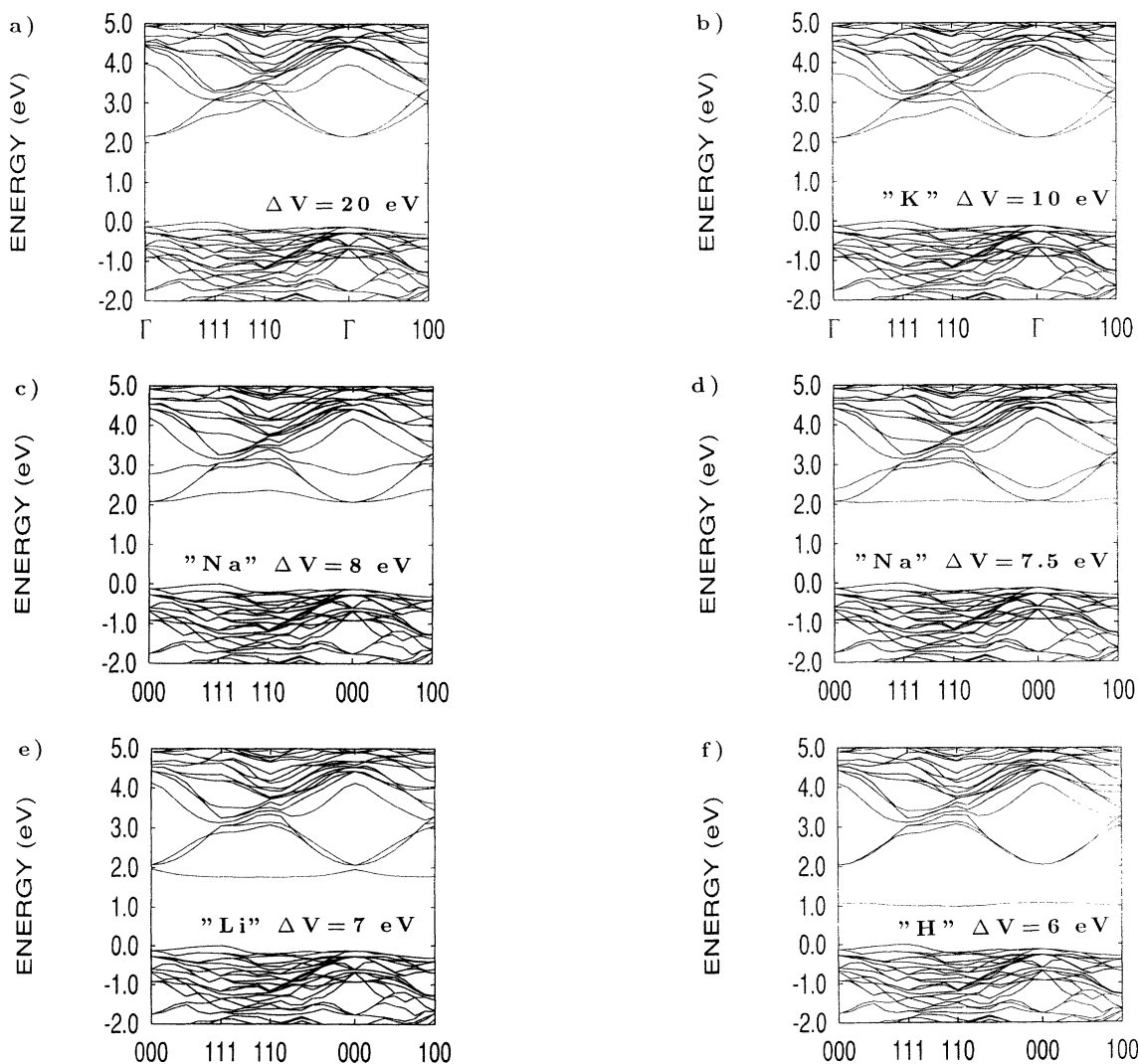


FIG. 5. The evolution of the band structure with the electropositivity (the on-site energy shift) of the doping atom. (a) $\Delta V_{\text{on-site}}=20$ eV, the lowest conduction band retains the general features of the pure Si(34). (b) $\Delta V_{\text{on-site}}=10$ eV, this shift may be interpreted as a "pseudo-K." (c) and (d) $\Delta V_{\text{on-site}}=8$ eV and $\Delta V_{\text{on-site}}=7.5$ eV, these shifts may be interpreted as a "pseudo-Na." (e) $\Delta V_{\text{on-site}}=7$ eV, this shift may be interpreted as a "pseudo-Li." (f) $\Delta V_{\text{on-site}}=6$ eV, this shift may be interpreted as a "pseudo-H."

“pseudo-Na.” Lowering the on-site energy shift further to 7.0 eV (“pseudo-Li”), we see the picture changes to one where the lowest conduction band state moves down into the “gap” [Fig. 5(e)]. Now it has definite A_1 symmetry at the Γ point. Finally, for the shift of 6.0 eV (an LDA “pseudo-H”), we get a flat nondegenerate band in the middle of the “gap” [Fig. 5(f)].

Now we discuss the $\text{Na}_8\text{Si}_{136}$ clathrate. We occupy every hexakaidecahedron and using the “pseudoatom” technique described above obtain the band structure shown in Fig. 6. The main effects are the small dispersion of a fully occupied lowest conduction band, and the appearance of a new band in the lower conduction band region at about 2.6 eV at Γ . This “new” state pushes the A type state brought down by the first sodium even further down in energy the effect is less pronounced in the region from (110) to Γ to (100) of the Brillouin zone.

To get a better understanding of the interaction between the two interstitials, and the effect the second sodium atom has on the band structure, we performed another calculation in the spirit of that presented in Fig. 4. We keep the on-site potential of one interstitial fixed at 7.5 eV (appropriate to Na), change the on-site shift of the second interstitial atom in the adjacent hexakaidecahedron, and monitor the energy eigenvalues at the Γ point. Results of this calculation are shown in Fig. 7. We see that the upper A type state comes down in energy as we reduce the on-site shift toward that of Na (7.5 eV). The lower state is unaffected until the shifts at both sites are equal, where the repulsion between the two A levels causes the lowest one to bend down. A similar effect has been predicted for chalcogen pairs in silicon.¹⁵ A peculiar implication of this result is that in the case of combined doping with two alkali metals, the least electropositive element has the dominant effect on the band structure.

Though our present modification of the Snakey-Niklewski method is done in the spirit of the empirical tight-binding method, we emphasize the importance of using a genuine first-principles scheme for calculations in this particular system. Being a low density phase of Si (the volume per atom in the clathrate phase is about 17% larger than that in the diamond phase), clathrate structures provide yet another example of the well known transferability problem in empirical tight binding. We il-

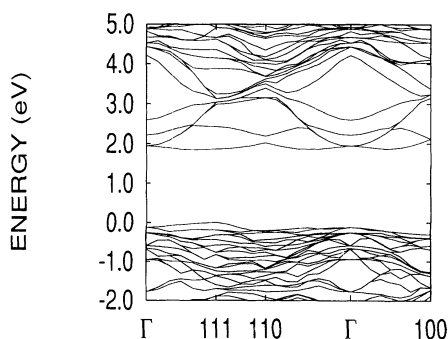


FIG. 6. The band structure in the near-band-gap region of $\text{Na}_8\text{Si}_{136}$ computed using the “pseudoatom” method.

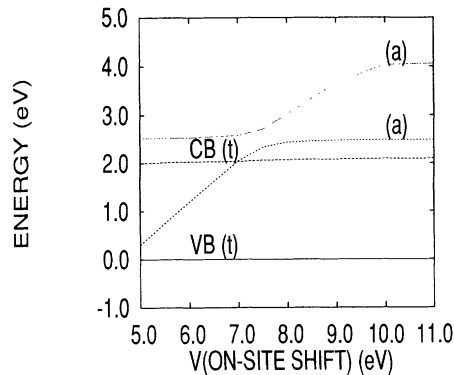


FIG. 7. The eigenstates in the near-gap region at the Γ point as a function of the on-site energy shift $\Delta V_{\text{on-site}}$ of the second interstitial atom in the adjacent hexakaidecahedron, when the on-site potential of the first interstitial is fixed at 7.5 eV, appropriate to Na.

lustrate this point in Fig. 8, where we show the energy per atom in eV as a function of the relative volume per atom for five different structures of silicon. This calculation was done using the tight-binding model of Goodwin *et al.*¹⁶ The most important feature of this figure is that while giving good results for the higher density phases of silicon (β tin, simple cubic, and fcc) which the model was specifically designed to do, the model predicts the clathrate phase to be the ground state. An identical problem exists in the Xu *et al.*¹⁷ empirical tight-binding model for carbon clathrates. Our previous calculations⁵ show that the Snakey-Niklewski technique does not have this difficulty, which gives us confidence in the interpretation of the results of the model calculations above.

To summarize this section, we find that the electronic properties of the Si clathrates may be altered in a controllable fashion by doping with alkali metals. The effect of doping on the band structure is stronger for less electropositive metals. Specifically, we find that doping with Na introduces a narrow band, which comes from the lowest conduction band in the pure Si material and retains the degeneracy at the Γ point [Fig. 5(c), 5(d)]. This band

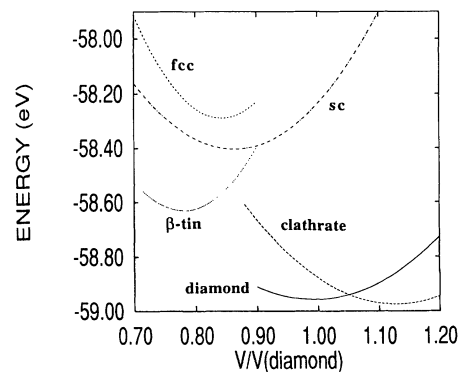


FIG. 8. Energy per atom in eV as a function of the relative volume per atom for five different structures of silicon (diamond, β -tin, sc, fcc, and clathrate). The calculation is done using the tight-binding model of Goodwin *et al.* (Ref. 16).

is half occupied at low sodium concentrations ($\text{Na}_4\text{Si}_{136}$), and fully occupied at higher concentrations ($\text{Na}_8\text{Si}_{136}$). For K doping, we predict that the effect should be less pronounced, and the lowest conduction bands will have structure similar to that of the pure Si material [Fig. 5(b)]. The degeneracy at the Γ point suggests a Jahn-Teller instability of the clathrate phase of Si doped with Na and K. This effect is discussed in the next section.

III. JAHN-TELLER EFFECT IN SOLID $\text{Si}(34)$

To study the Jahn-Teller effect in the $M_4\text{Si}_{136}$ (M stands for the alkali-metal atom) system, we use the following method. First, to describe the doping effect, we introduce the interstitial “pseudo-alkali-metal atom” in the center of the hexakaidecahedron as described in the previous section. The choice of the on-site shift for the interstitial depends on which atom we wish to simulate. We then perform a quantum molecular dynamics (QMD) relaxation of the structure [Si(34) plus the interstitial with the proper number of electrons], the details of the QMD technique are described in Ref. 13. During the QMD run, the atoms are free to move in the direction of the forces (in the presence of a fictitious damping), until the zero-force (relaxed) configuration is achieved. In these simulations, we use 216 special k points for the integration over the Brillouin zone since the material will generally be metallic and have no symmetry. If done at zero temperature, the first few QMD steps tend to produce a totally symmetric distortion. Several room temperature vibrations are used to break the symmetry and the energy is reduced further as the system is quenched to the zero-force configuration. This zero-force configuration is lower in energy than the initial unrelaxed solid with the interstitial, and we refer to the difference in these two energies as the JT distortion energy, E_{JT} [thus the energy of the totally symmetric (A -type) relaxation is also included].

First we examine the Jahn-Teller effect for the case of Na doping ($\text{Na}_4\text{Si}_{136}$). Based on the discussion in the previous section, to reproduce the effect of Na on the band structure, we choose the on-site shift of 7.5 eV for the interstitial atom. It must be stated, that our JT energies are only estimates, because of the use of the “pseudo-Na” atom approximation for the QMD.

By symmetry there are multiple equivalent Jahn-Teller distortions. The QMD relaxation finds repeatedly a small atomic displacement. In any of the multiple minima, the JT distortion energy is $E_{JT}=99.6$ meV/cell; this is small if compared with that in the hypothetical fullerene solid C_{20} , where the JT energy is 1.759 eV/ball.¹⁸ As for the atomic geometry, the main effect is that the “pseudo-Na” atom moves away from the center of the 28 atom cage by 0.17 Å. Displacements of the other atoms in the unit cell are significantly smaller. The analysis of these atomic displacements shows that as a result of the JT distortion, the site symmetry was reduced from T_d to C_{3v} .

The band structure calculated for the final configuration is shown in the Fig. 9. The relaxation lifts the degeneracy at the Γ point, and the lowest conduction band

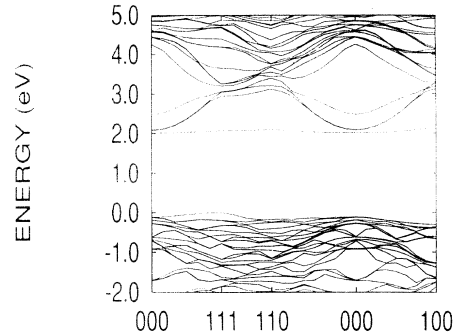


FIG. 9. The band structure calculated for the final JT relaxed configuration of $\text{Na}_4\text{Si}_{136}$ using the “pseudoatom” method. The relaxation lifts the degeneracy at the Γ point, and the lowest conduction band edge is moved further down into the “gap.” The JT gap (at $k = \Gamma$) $\Delta_{JT}=0.065$ eV.

edge is moved further down into the “gap.” The JT gap (at $k = \Gamma$) is $\Delta_{JT}=0.065$ eV. However, because of the limitations imposed by a single particle theory (LDA) that we are using, we cannot address the undoubtedly important electronic correlation effects in this narrow metallic band at the level which they deserve in this paper.

We now discuss the Jahn-Teller effect for K doped Si(34). The band structure for this material without JT distortion is shown in Fig. 5(b). The highest occupied band of the doped unrelaxed solid retains most of the free-electron character of the conduction band of the pure Si material. We estimate the effective mass in this metallic band in the (100) direction to be $0.58m_e$.

Because the band structure of the unrelaxed material doped with potassium is similar to that of the pure Si material, it is reasonable to conclude that the main effect of the potassium atom on the electronic structure is to donate an electron to the conduction band, similar to the effect alkali-metal doping has in carbon fullerene solids. To exploit this similarity, we first did the calculation using the method introduced in (Ref. 18) for fullerene molecules and solids which become JT unstable when negatively charged. The effect of doping is simulated in this technique by adding n electrons to the relaxed Si(34) solid configuration, or “charging” the solid negatively. First, we perform a QMD simulation to obtain the relaxed configuration of the neutral undoped Si(34) solid. The final relaxed configuration of this run becomes the initial configuration for the QMD simulation of the “doped” solid, which contains the dopant electron. Because the conduction band of Si(34) is triply degenerate at the Γ point, the negatively “charged” structure is JT unstable. We now subject the resulting $\text{Si}(34)^{-n}$ to a final QMD relaxation. Again several initial room temperature vibrations are required to break the symmetry, and the rest of the calculation is exactly as the one described above. For $n = 1$ (simulating $\text{K}_4\text{Si}_{136}$), we obtain $E_{JT}=52$ meV/cell, and the JT gap (at $k = \Gamma$) $\Delta_{JT}=0.145$ eV. The corresponding band structure is shown in Fig. 10, and demonstrates the splitting of the conduction band edge at the Γ point, and the almost uniform downshift of the lowest conduction band as a result of the JT distortion. The charge den-

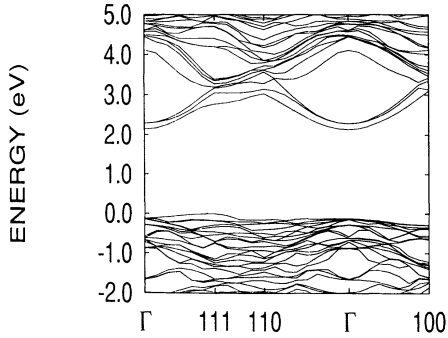


FIG. 10. The band structure calculated for the final JT relaxed configuration of K_4Si_{136} using the “doping electron” method (Ref. 18). As a result of a Jahn-Teller distortion the degeneracy at the Γ point has been lifted and the entire lowest conduction band moved down in energy with the JT gap (at $k = \Gamma$) being $\Delta_{JT} = 0.145$ eV.

sity of the added electron ($n=1$) is found to be equally distributed among all the atoms in the unit cell, and is predominantly p type. We have also repeated the calculation putting in “pseudo-K,” and find nearly identical results to those just described. Ordering may change the symmetry and result in a small splitting of the levels, but we believe that this effect will be smaller than the Jahn-Teller effect.

We conclude that in the alkali-metal-doped silicon clathrates the JT distortion lifts the degeneracy of the lowest conduction band and produces a flat band separated from delocalized states by a gap of ≈ 0.065 eV. Specifically, we find Na_4Si_{136} to be a metal with a very narrow conduction band, and a full understanding of its properties can only be addressed by methods beyond those of single particle theory.

IV. DISCUSSION

We now briefly discuss the insulator-to-metal transition in Na doped Si clathrates. An early qualitative discussion of such a transition in Na_xSi_{136} was given by Mott.⁹ We review the main points of his description first. Following Cros *et al.*,¹⁰ Mott assumed that the electrons move in a “sodium band” which is similar to the impurity band one may observe in Si:P when the phosphorus concentration is high. He assumed that the band should lie well below the conduction band edge because the electron coming from the sodium atom is underscreened according to the effective mass theory, and, therefore, the conduction band states can be excluded from the picture. As the sodium concentration is decreased, the electron gas in the “sodium band” undergoes three phase transitions from the highly-correlated nonmagnetic metal to the antiferromagnetic metal, and finally *via* Mott transition to the antiferromagnetic insulator.

Our calculations do not cover the whole concentration range discussed by Mott, but suggest a somewhat different picture. We have shown, that at the lower sodium concentrations, when just one sodium atom is introduced

into the unit cell, there are no electronic states present in the gap. The highest occupied band shows very little dispersion and is triply degenerate at the Γ point. This leads to a Jahn-Teller distortion which results in a split-off narrow nondegenerate half-filled band in the “gap.” The nature of this band is quite different from the impurity band proposed by Mott. The charge density is not localized on the Na atom, but rather distributed over the Si atoms forming the hexakaidecahedral cage surrounding the interstitial. In the ideal $Si(34)$ structure, these Si atoms give rise to a bundle of the nearly degenerate states in the conduction band at about 3 eV. Even though the energy difference between the Na state and the Si states is large (≈ 5 eV), the wave function overlap is significant (the radius of the cage is about 4.0 Å, and the 3s wave function of Na at this radius is about 28% of its’ peak value). This overlap introduces an additional weak interaction between the states in the bundle *via* hopping on and off the interstitial. This interaction results in the splitting off of a symmetric state from the bundle, and this mechanism is identical to a special eigenstate problem discussed by Kittel.¹⁹ The highest occupied band flattens out and remains triply degenerate at the Γ point. This leads to a Jahn-Teller distortion which results in a split-off narrow nondegenerate half filled band in the “gap.”

We may obtain a rough estimate of the electron-electron electrostatic repulsion U , by using $U = \frac{1}{4\pi\epsilon_0} \frac{3e^2}{5A}$ (Coulomb self-interaction of a uniformly charged sphere of radius A), where A is a measure of the electron localization. Using $A=5.0$ Å (the extent of the Na 3s wave function), we obtain $U = 1.73$ eV. The width of the metallic band W is of the order of 0.1 eV. Then, for the Mott parameter W/U , we obtain ≈ 0.06 , which supports a concept of nonmetallic Mott-Hubbard state for Na_4Si_{136} clathrate. The estimate though should be taken cautiously, because when the material dielectric constant is used the result may change up to an order of magnitude. Using similar arguments, we may suggest that it may be possible that in Na_8Si_{136} the strong electrostatic repulsion excites an electron over the JT gap into the next conduction band making this system a correlation induced metal.^{20,21}

We now discuss the possible ways of band-gap engineering in Si based materials. A significant increase of the optical band gap has been recently reported in a variety of silicon based materials and nanostructures. Frequently, the explanation of this effect is based on quantum confinement effects. Furukawa and Miyasato reported a wide optical band gap of 2.4 eV in a microcrystalline Si:H fabricated by planar magnetron rf sputtering in hydrogen gas onto a Si substrate.²² They explained the widening of the gap by a three-dimensional quantum-well effect. Canham found strong visible photoluminescence (1.76 eV) in anodically etched (“porous”) silicon, and attributed it to the quantum confinement effect.²³ Kanemitsu, Ogawa, Shiraishi, and Takeda reported strong visible photoluminescence (1.65 eV) in the Si nanometer-sized spheres produced by laser breakdown of silane gas.²⁴ They explained this effect by the exciton confinement on a nanometer-sized spherical shell. This list is far from complete. A number of theoret-

ical calculations for H-terminated Si wires have been performed.²⁵⁻²⁷ The wire diameter necessary to reproduce the luminescence peak ranges from 15 Å to 30 Å in these calculations. However, these diameters appear to be about an order of magnitude smaller than the typical size suggested by electron microscopy.²⁸ Models alternative to the quantum confinement theory have also been proposed. Brandt, Fuchs, Stutzmann, Weber, and Cardona have proposed that the luminescence in porous silicon was from siloxene derivatives present in this material.²⁹ In their interpretation, specific chemical reactions between silicon, oxygen, and hydrogen define the luminescence properties of the material.

What silicon clathrates have in common with these systems is a wide (1.9 eV) indirect optical band gap. However, the opening of the gap in the clathrates has nothing to do with the confinement effect, but rather is caused by the slight bending and stretching of silicon bonds compared to the diamond phase. Thus, silicon clathrate structures suggest an alternative way of gap engineering, which does not require either quantum confinement effect or the presence of oxygen in the material.

V. CONCLUSIONS

In conclusion, we have studied theoretically the effects of alkali-metal doping in clathrate Si solids. We find that different metals have different effects on the lowest conduction band states. At low concentrations, the resulting compounds are metallic in a one electron picture. However, for Na doping, we find a flat band and Jahn-Teller distorted band, which may produce an insulating structure when many electron effects are included. Formation of the insulating state is probably due to a combination of the Jahn-Teller and Mott transitions.

ACKNOWLEDGMENTS

We thank the Office of Naval Research (Contract No. ONR N00014-90-J-1304) and the NSF high pressure material synthesis MRG (DMR-9121570) for support. A.A.D. would like to thank Dr. Oleg Pankratov and Professor J. B. Page for the insightful discussions. We also thank Dr. Jan Gryko and Professor Paul McMillan for their efforts in synthesizing the material.

¹ H. Davy, *Philos. Trans. R. Soc. London* **101**, 30 (1811).

² M. Faraday, *Quart. J. Sci.* **15**, 75 (1823).

³ C. Cros, M. Pouchard, and P. Hagenmuller, *C. R. Acad. Sci.* **260**, 4764 (1965).

⁴ S. B. Roy, K. E. Sim, and A. D. Caplin, *Philos. Mag. B* **65**, 1445 (1992).

⁵ G. B. Adams, M. O'Keeffe, A. A. Demkov, O. F. Sankey, and Y.-M. Huang, *Phys. Rev. B* **49**, 8048 (1994).

⁶ R. Nesper, K. Vogel, and P. Blochl, *Angew. Chem.* **32**, 701 (1993).

⁷ M. O'Keeffe, G. Adams, and O. Sankey, *Phys. Rev. Lett.* **68**, 2325 (1992).

⁸ M. Martin, D. Koller, X. Du, P. Stephens, and L. Mihaly, *Phys. Rev. B* **49**, 10818 (1994).

⁹ N. F. Mott, *J. Solid State Chem.* **6**, 348 (1973).

¹⁰ C. Cros, M. Pouchard, and P. Hagenmuller, *J. Solid State Chem.* **2**, 570 (1970).

¹¹ G. Kerker, *J. Phys. C* **13**, 189 (1980).

¹² M. Troullier and J. L. Martins, *Phys. Rev. B* **43**, 1993 (1991).

¹³ O. F. Sankey and D. J. Niklewski, *Phys. Rev. B* **40**, 3979 (1989).

¹⁴ E. Clementi and C. Roetti, *At. Data Nucl. Data Tables* **14**, 177 (1974).

¹⁵ O. F. Sankey and J. D. Dow, *Solid State Commun.* **50**, 705 (1984).

¹⁶ L. Goodwin, A. Skinner, and D. Pettifor, *Europhys. Lett.* **9**, 701 (1989).

¹⁷ C. Xu, C. Wang, C. T. Chan, and K. Ito, *J. Phys. Condens. Matter* **4**, 6047 (1992).

¹⁸ G. Adams, O. Sankey, and J. P. Page, *Chem. Phys.* **176**, 61 (1993).

¹⁹ C. Kittel, *Introduction to Solid State Physics* (Wiley, New York, 1971), p. 744.

²⁰ Q. Si, M. Rozenberg, G. Kotliar, and A. E. Ruckenstein, *Phys. Rev. Lett.* **72**, 2761 (1994).

²¹ G. Aeppli and Z. Fisk, *Comments Condens. Matter Phys.* **16**, 155 (1992).

²² S. Furukawa and T. Miyasato, *Phys. Rev. B* **38**, 5726 (1988).

²³ L. Canham, *Appl. Phys. Lett.* **57**, 1046 (1990).

²⁴ Y. Kanemitsu, T. Ogawa, K. Shiraishi, and K. Takeda, *Phys. Rev. B* **48**, 4883 (1993).

²⁵ G. Sanders and Y.-C. Chang, *Phys. Rev. B* **45**, 9202 (1992).

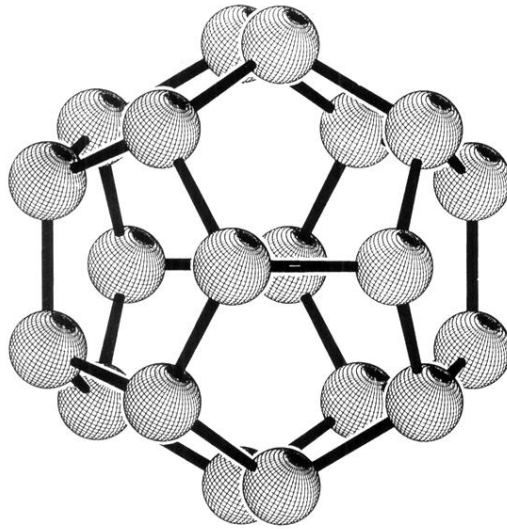
²⁶ A. Read, R. Needs, and K. Nash, *Phys. Rev. Lett.* **69**, 1232 (1992).

²⁷ F. Buda, J. Kohanoff, and M. Parrinello, *Phys. Rev. Lett.* **69**, 1272 (1992).

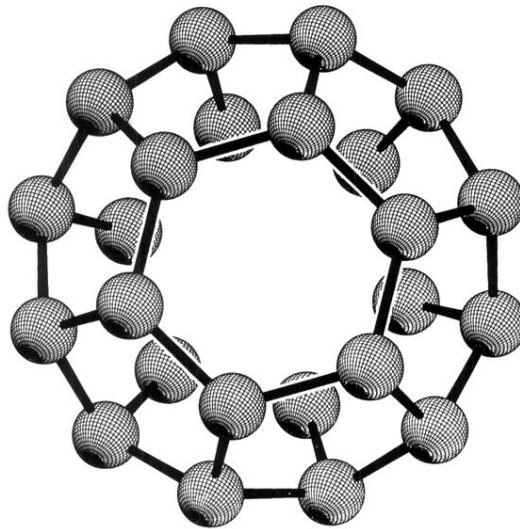
²⁸ M. I. J. Beale, N. G. Chew, M. J. Uren, A. G. Cullis, and J. D. Benjamin, *Appl. Phys. Lett.* **46**, 86 (1985).

²⁹ M. Brandt, H. Fuchs, M. Stutzmann, J. Weber, and M. Cardona, *Solid State Commun.* **81**, 307 (1992).

a)



b)



c)

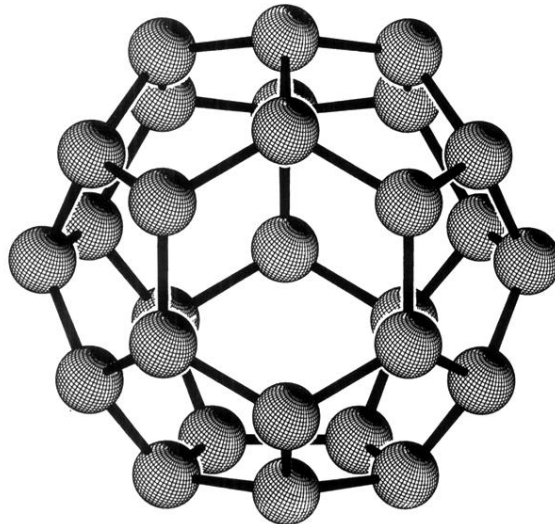


FIG. 1. The building blocks of the silicon clathrate structures: (a) pentagonal dodecahedron, (b) tetrakaidecahedron, and (c) hexakaidecahedron.

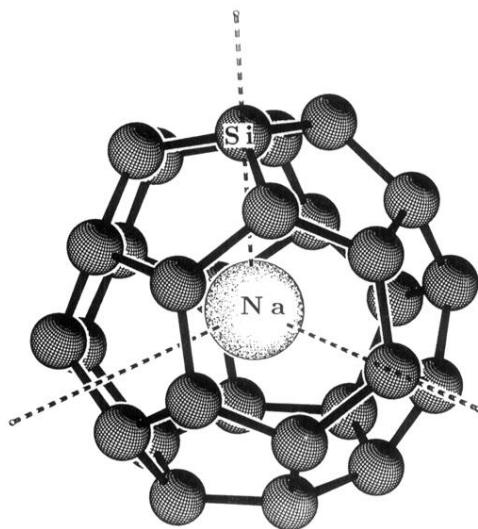


FIG. 2. A Na atom in the center of the Si hexakaidecahedron. This site has a perfect T_d symmetry.